

Article

# Immobilised Cerium-Doped Zinc Oxide as a Photocatalyst for the Degradation of Antibiotics and the Inactivation of Antibiotic-Resistant Bacteria

Ian Zammit <sup>1</sup>, Vincenzo Vaiano <sup>2</sup>, Ana R. Ribeiro <sup>3</sup>, Adrián M. T. Silva <sup>3</sup>, Célia M. Manaia <sup>4</sup> and Luigi Rizzo <sup>1,\*</sup>

<sup>1</sup> Department of Civil Engineering, University of Salerno, Via Giovanni Paolo II 132, 84084 Fisciano, Italy; izammit@unisa.it

<sup>2</sup> Department of Industrial Engineering, University of Salerno, Via Giovanni Paolo II 132, 84084 Fisciano, Italy; vvaiano@unisa.it

<sup>3</sup> Laboratory of Separation and Reaction Engineering-Laboratory of Catalysis and Materials (LSRE-LCM), Faculdade de Engenharia, Universidade do Porto, Rua Dr. Roberto Frias, 4200-465 Porto, Portugal; ritalado@fe.up.pt (A.R.R.); adrian@fe.up.pt (A.M.T.S.)

<sup>4</sup> Universidade Católica Portuguesa, CBQF-Centro de Biotecnologia e Química Fina – Laboratório Associado, Escola Superior de Biotecnologia, Rua Arquiteto Lobão Vital, 172, 4200-374 Porto, Portugal; cmanaia@porto.ucp.pt

\* Correspondence: l.rizzo@unisa.it; Tel.: +39-089969334; Fax: +39-089969620

Received: 28 January 2019; Accepted: 19 February 2019; Published: 1 March 2019



**Abstract:** The threat of antibiotic resistance to the wellbeing of societies is well established. Urban wastewater treatment plants (UWTPs) are recognised sources for antibiotic resistance dissemination in the environment. Herein a novel cerium-doped zinc oxide (Ce-ZnO) photocatalyst is compared to ZnO and the benchmark TiO<sub>2</sub>-P25 in the immobilised form on a metallic support, to evaluate a photocatalytic process as a possible tertiary treatment in UWTPs. The catalysts were compared for the removal of two antibiotics, trimethoprim (TMP) and sulfamethoxazole (SMX), and for the inactivation of *Escherichia coli* (*E. coli*) strain DH5-Alpha in isotonic sodium chloride solution and of autochthonous bacteria in real secondary wastewater. In real wastewater, *E. coli* and other coliforms were monitored, as well as the respective fractions resistant to ofloxacin and azithromycin. In parallel, *Pseudomonas aeruginosa* and the respective sub-population resistant to ofloxacin or ciprofloxacin were also monitored. Photocatalysis with both ZnO and Ce-ZnO was faster than using TiO<sub>2</sub>-P25 at degrading the antibiotics, with Ce-ZnO the fastest against SMX but slower than undoped ZnO in the removal of TMP. Ce-ZnO catalyst reuse in the immobilised form produced somewhat slower kinetics maintained >50% of the initial activity, even after five cycles of use. Approximately 3 log<sub>10</sub> inactivation of *E. coli* in isotonic sodium chloride water was recorded with reproducible results. In the removal of autochthonous bacteria in real wastewater, Ce-ZnO performed better (more than 2 log values higher) than TiO<sub>2</sub>-P25. In all cases, *E. coli* and other coliforms, including their resistant subpopulations, were inactivated at a higher rate than *P. aeruginosa*. With short reaction times no evidence for enrichment of resistance was observed, yet with extended reaction times low levels of bacterial loads were not further inactivated. Overall, Ce-ZnO is an easy and cheap photocatalyst to produce and immobilise and the one that showed higher activity than the industry standard TiO<sub>2</sub>-P25 against the tested antibiotics and bacteria, including antibiotic-resistant bacteria.

**Keywords:** antibiotic resistance; immobilised photocatalyst; photocatalysis; tertiary treatment; wastewater disinfection

## 1. Introduction

The efficacy of antibiotics in treating bacterial infections is dwindling due to an increase in antibiotic resistance (AR). Nowadays, the threat of AR to the health, wellbeing and economy are well recognised, which in the future may represent a global problem with hundreds of thousands of people dying from resistant pathogens and billions of dollars in economic losses [1].

Antibiotic resistance is not confined to the clinical setting. Regarding environmental compartments, urban wastewater treatment plants (UWTPs) are well established as point sources for the spread and release of antibiotics, antibiotic-resistant bacteria (ARB) and antibiotic resistant genes into the environment [2]. Despite this, there are many knowledge gaps pertaining both to environmental dissemination of AR after wastewater discharge [3,4] and to treatment technologies that are correlated with low AR prevalence [5], i.e., those feasible to be engineered with the aim of mitigating AR release.

The concern is that the environmental resistome acts as a source of AR to the clinical resistome [6], and a higher prevalence of resistance in the environment, which is due to anthropogenic action, implies a higher risk of transfer to the clinical settings. This concern is further compounded by the projected increase in water stress due to climate change and population growth [7]. Water reuse, especially for agricultural irrigation, is considered as a necessary approach for future water management and is actively promoted by the European Commission [8,9]. While current UWTPs may include a disinfection step to meet regulations dealing with bacterial load before discharge or reuse, they are not designed to specifically tackle the AR problem. Since AR mitigation is not a direct target of wastewater treatment, there is a possibility that treatment while promoting the reduction of AR does not guarantee the adequate reduction of the relative abundance of AR [10].

Chlorination, the most widely applied disinfection treatment in UWTPs, and UVC disinfection have been both linked to an increase in prevalence of AR [10–12]. Ozonation, which is considered as the treatment of choice to meet newer strict regulatory requirements in terms of micropollutant emissions, has also been associated with AR prevalence increase [13]. A potential alternative treatment process to current technologies is heterogeneous photocatalysis (HPC), an advanced oxidation process (AOP) which can oxidise a wide range of chemical contaminants, as well as inactivate microorganisms due to the formation of different radical species [14,15]. While also being an oxidative process, HPC is not associated with the formation of toxic disinfection by-products, such as is the case for chlorination [16] and ozonation [17]. The use of HPC at real scale has, however, been limited by its cost and the lack of more stringent regulations on the quality of UWTP effluents to address new challenges (such as the removal of contaminants of emerging concern). With more stringent regulations, HPC could be possibly regarded as an economically feasible and competitive technology when compared to consolidated tertiary treatment technologies [18].

Photocatalyst immobilisation, i.e., having the photocatalyst on a support as opposed to a powder in suspension, has been previously proposed by a number of authors [19–21]. Immobilisation has been suggested to not negatively affect bacterial inactivation rates cf. suspension, since any lower activity due to immobilisation is compensated by the activity being concentrated on a smaller area of the bacteria cell wall, which results in reaching the inactivation threshold earlier [21,22]. However, the majority of published articles dealing with immobilised photocatalysts are focused on TiO<sub>2</sub>. Other photocatalysts, such as ZnO, are less reported in the literature [23–25].

In an effort to develop a photocatalytic reactor, which is feasible for large scale wastewater tertiary treatment, a ZnO-based catalyst doped with cerium was previously optimised [26]. To reduce operating costs associated with having the catalyst in powder form (such as agitation needed to keep the catalyst in suspension, requirement of catalyst recovery and its partial loss with the effluent), the photocatalyst is herein immobilised on a mechanically-treated stainless steel surface with a silica interlayer. The photocatalytic activity of the immobilised cerium-doped ZnO catalyst (Ce-ZnO) is investigated for the possible development of a tertiary treatment of urban wastewater in the oxidation of chemical species (antibiotics) and inactivation of bacteria, including specifically

putative antibiotic-resistant bacteria. The target antibiotics were previously prioritised as model antibiotics within the ANSWER project (H2020-MSCA-ITN-2015 number 675530) and NEREUS COST Action (Cost Action ES1403). The prioritisation, amongst other parameters, is based on their potential for crop uptake, persistence and widespread use [27]. Specifically, the photocatalytic degradation of trimethoprim (TMP) and sulfamethoxazole (SMX) in pure water was studied, as well as the wastewater autochthonous resistance of coliforms and *Pseudomonas aeruginosa* to ofloxacin, azithromycin, or ciprofloxacin. It is worth mentioning that doped and undoped ZnO were directly benchmarked against TiO<sub>2</sub>-P25. Finally, to the authors' knowledge, there is no application available in the scientific literature of immobilised ZnO-based catalysts against antibiotic-resistant bacteria.

## 2. Results and Discussion

### 2.1. Photocatalyst Immobilisation and Characterisation

The outlined procedure was successful in producing a coating that did not flake off when submerged in water and produced discs that were reusable without any recovery steps. The silica interlayer deposition and corresponding light microscope magnification is shown in Figure 1A, whereas Figure 1B shows the photocatalyst coated on the interlayer.

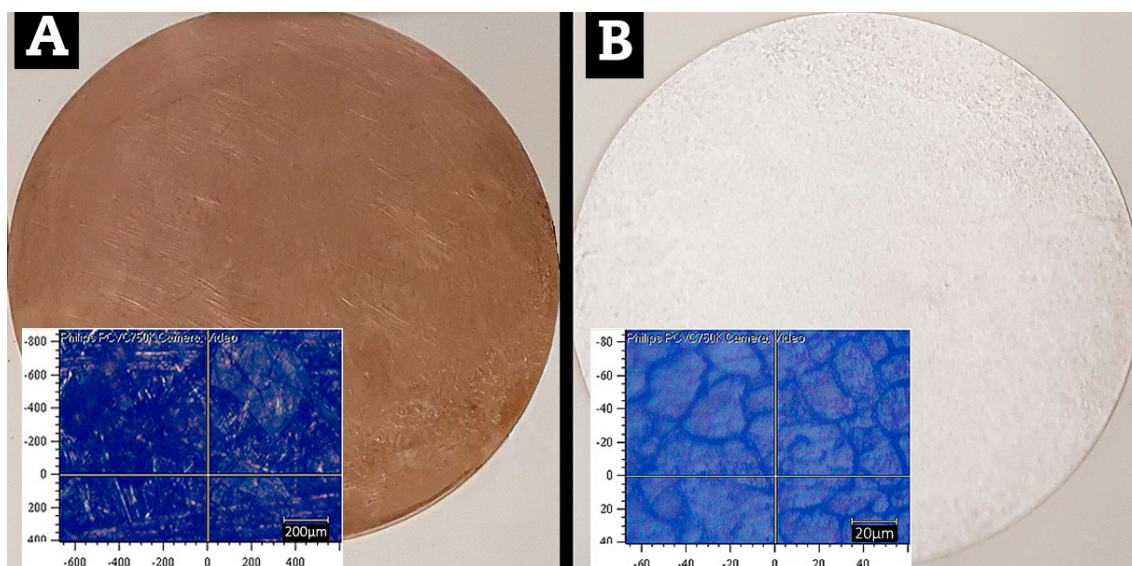


**Figure 1.** (A) Disc after silica interlayer coating and (B) after Ce-ZnO coating—both with optical microscopy images inset.

XRD patterns obtained for the SiO<sub>2</sub> disc, 304SS (steel substrate), Ce-ZnO disc and Ce-ZnO powder are shown in Figure 2.

The uncoated metal disc, referred to as 304 SS, shows signals at  $2\theta$  of about  $43^\circ$ ,  $45^\circ$ ,  $51^\circ$  and  $75^\circ$  due to the steel crystalline structure [28–30]. The Ce-ZnO disc additionally presented all the diffraction peaks observed for Ce-ZnO powder ( $2\theta$  at  $31.7^\circ$ ,  $34.4^\circ$ ,  $36.2^\circ$ ,  $47.7^\circ$ ,  $56.5^\circ$ ,  $62.7^\circ$ ,  $68.4^\circ$  corresponding to (100), (002), (101), (102), (110), (103) and (112) planes, respectively) due to the typical hexagonal wurtzite structure of ZnO [26]. This confirms that the coating of the steel surface by Ce-ZnO particles was in fact cerium-doped ZnO. This very simple method of coating has the potential to reduce operating costs of photocatalytic systems, namely by extending the usability of the catalyst and by not requiring post-treatment steps to separate the photocatalyst from the tertiary treated wastewater.

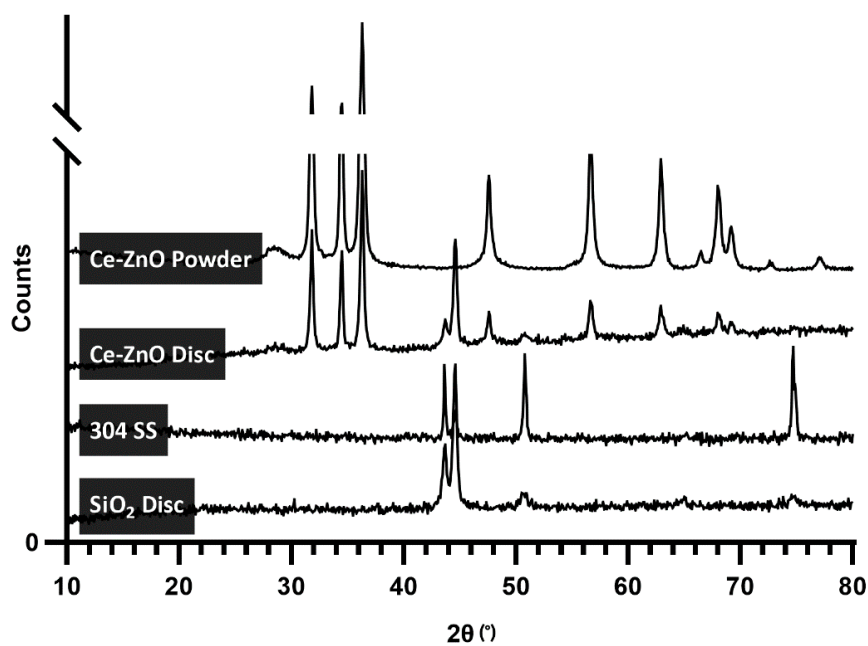


Figure 2. XRD patterns of SiO<sub>2</sub> disc, 304SS (bare metal disc), Ce-ZnO disc and Ce-ZnO powder.

## 2.2. Photocatalytic Degradation of Antibiotics

The three immobilised photocatalysts were effective in degrading the investigated antibiotics. Figure 3 shows the linear fit corresponding to pseudo-first-order reaction kinetics. Statistics (standard error and R<sup>2</sup>) and kinetic parameters (pseudo first-order rate constant ( $k$ ) and half-life time ( $t_{1/2}$ )) are included in Table 1.

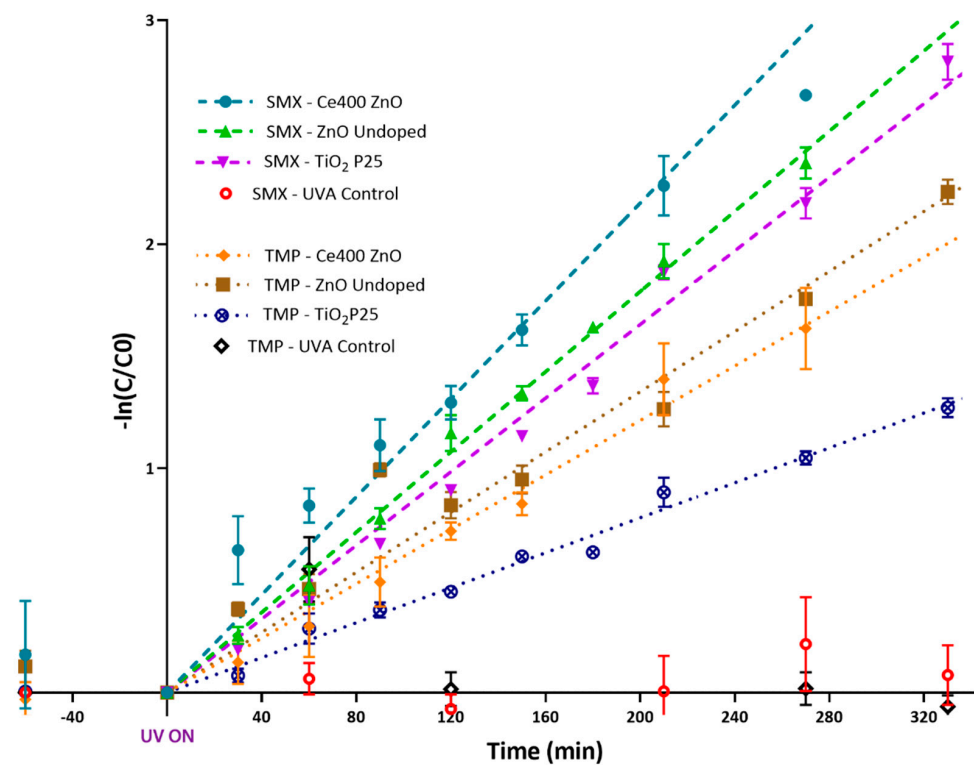


Figure 3. Pseudo first-order plots for the degradation of SMX and TMP with immobilised catalysts.

**Table 1.** Linear regression equations of Figure 3.

	SMX				TMP			
	Ce400 ZnO	ZnO Undoped	TiO <sub>2</sub> P25	UVA Control	Ce400 ZnO	ZnO Undoped	TiO <sub>2</sub> P25	UVA Control
Std. Error	$2.63 \times 10^{-4}$	$8.80 \times 10^{-5}$	$9.90 \times 10^{-5}$	$1.52 \times 10^{-4}$	$1.44 \times 10^{-4}$	$1.79 \times 10^{-4}$	$5.50 \times 10^{-5}$	$3.32 \times 10^{-4}$
R <sup>2</sup>	0.943	0.993	0.988	0.083	0.956	0.941	0.983	-0.248
<i>k</i> (min <sup>-1</sup> )	$1.09 \times 10^{-2}$	$8.95 \times 10^{-3}$	$8.21 \times 10^{-3}$	$3.28 \times 10^{-4}$	$6.07 \times 10^{-3}$	$6.71 \times 10^{-3}$	$3.90 \times 10^{-3}$	$9.45 \times 10^{-5}$
<i>t</i> <sub>1/2</sub> (min)	63.6	77.4	84.4	2113.3	114.2	103.3	177.7	7334.9

The contribution of adsorption process to SMX and TMP removals accounted for less than 10% for all the photocatalysts investigated. SMX was less persistent than TMP, all three photocatalysts degrading SMX faster than TMP. Among the different photocatalysts, the slowest removal for both antibiotics was obtained with TiO<sub>2</sub>-P25. Ce-ZnO performed better than undoped ZnO in the removal of SMX, but the opposite was observed for TMP.

The experimentally measured hydroxyl radical rate constant ( $\log k_{OH}$ ) with SMX is 9.76 [31] while that for TMP is 9.84 [32]. Thus, if the reaction was exclusively based on free-form hydroxyl radicals, the competitive kinetics would dictate a degradation rate of SMX being approx. 84% of the rate for TMP. The discrepancy (i.e., the fact that TMP was not degraded faster than SMX with both photocatalysts) implies that other processes and reactions, apart from hydroxyl radical-induced oxidation, are involved. The other reactive processes taking place could range from oxidation with other reactive oxygen species and/or direct reactions on the catalyst surface [33]. These reactions would be affected by the adsorption of specific compounds on the immobilised catalyst, including transformation products. Reactions on the photocatalytic surface would also explain why one catalyst is not the most effective at degrading both antibiotics. The different chemical structures result in different adsorption affinities and hence imply less probable reaction at the surface and slower removal rate. Thus, while efficiency in generation of reactive oxygen species (ROS) is of high importance in determining the efficacy of the photocatalysts, it is not the sole substantial contributor.

Reusability tests were also conducted with the Ce-ZnO coated disc (Figures 4 and 5 for SMX and TMP, respectively). No cleaning steps were undertaken, the disc was simply dried at 80 °C for 30 min and stored before the next experiment when it was reused. In the case of SMX (Figure 4), a partial drop in the removal rate (and respective pseudo first-order reaction rate constant) took place after the first use, but no major differences were observed from the second to the last (i.e., fifth) reutilization.

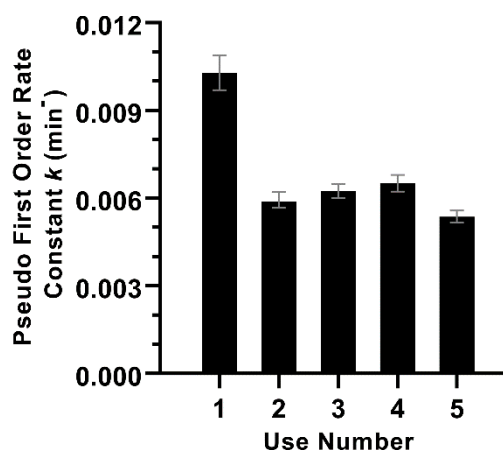


**Figure 4.** Reusability tests: pseudo first-order reaction rate constants for SMX experiments (i.e., the same coated disc was reused with 1 L of spiked water and 36 W UVA).

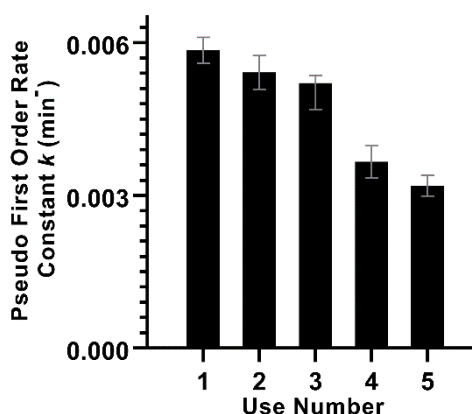


**Figure 5.** Reusability tests: pseudo first-order reaction rate constants for TMP experiments (i.e., the same coated disc was reused with 1 L of spiked water and 36 W UVA).

Regarding TMP (Figure 5), a more gradual decrease in the catalytic activity was observed when the catalyst was reused. However, no flaking-off of the catalyst from the disc into suspension was observed with the naked eye. ZnO photochemical corrosion was also not an issue as is expected in aqueous media close to neutral pH [34]. The reuse of photocatalysts, albeit not the specific cerium-doped ZnO used herein, was studied before in several reports. For instance, in a previously published work, although powder titania was reused in industrial dyes photocatalytic degradation tests, a decrease in performance was not observed [35]. In the same study, a negligible increase in the rate of removal of the dye at catalyst loads higher than 0.5 g/L was observed but the reuse at these lower catalyst loads was not investigated. The high catalyst load investigated as well as the fact that no rate increase above 0.5 g/L loadings was observed, suggest that catalyst poisoning could still be taking place, but its activity is taken up by the excess photocatalyst that was not being utilised at peak performance. Similarly, Rao et al. [36] reported no decrease in removal rates of salicylic acid with a high suspended catalyst load of 2 g/L, but only up to five reuse cycles after which a decrease in activity was reported. This supports the possibility that catalyst poisoning is taking place and being replaced by the unexploited excess. Fernández-Ibáñez et al. [37] reused two types of titania under solar illumination and at a suspended catalyst load of 0.2 g/L. At this much lower catalyst load, both catalysts gave decreasing removal rates with reuses, with one of the catalysts showing higher susceptibility to catalyst poisoning. ZnO reuse in powdered form was investigated by Chakrabarti and Dutta [38], which also showed major decreases in the removal rate (21% and 23% cf. 39% with the unused catalyst). At a moderately high catalyst load of 1.25 g/L, a low level of reduction in removal rates of methyl orange was observed for a glycerol scaffold-synthesised ZnO catalyst and somewhat higher reduction for TiO<sub>2</sub>-P25 [39]. Photocatalysts in the immobilised form are far less common in the literature, and many reports dealing with TiO<sub>2</sub> and ZnO immobilization do not report reuse efficiency of the immobilised photocatalyst [23,40–43], despite reusability being one of the main advantages of immobilised HPC over suspension based one [43]. Lalhriatpuia et al. [44] reported encouraging results of reusability of immobilised titania. This catalyst used five times against tetracycline and diclofenac showed minor reduction in removal rates for the former compound and low reduction of activity for the latter compound. The variation of the reactions rates with reuses, apart from initial catalyst load, are also dependent on the compound of interest. It is presumed that a compound that produces reaction products that have a higher affinity to the catalyst or absorb UV radiation to a higher extent will interfere with the photocatalytic process to a higher degree, thus resulting in a larger decrease in reaction rate with reuse cycles [45].

Outside the field of environmental catalysis, ZnO and other catalysts are used in organic synthesis for oxidation reactions, albeit their use is less widespread than in environmental remediation [46]. For ZnO as a classical chemical catalyst, it was observed that a simple ZnO washing with dichloromethane was sufficient to remove interfering agents, avoiding the decrease in the reaction rate with consecutive reuses [47]. For large scale application, keeping green chemistry principles in

mind, a non-chlorinated and hence greener solvent might also be suitable for catalyst regeneration, which would not be too laboursome if the catalyst is immobilised on a metallic surface, since plastic surfaces might not be compatible with many solvents.

### 2.3. Photocatalytic Inactivation of *E. coli* in Isotonic Saline Solution

The HPC treatment using the immobilised Ce-ZnO catalyst was also effective in the inactivation of *E. coli* in saline water (0.85% NaCl). As expected, the higher initial cell density (Figure 6 series A) needed longer reaction times for inactivation. Bacterial inactivation takes place via peroxidation of the bacteria's cell walls at multiple points [48]. With higher bacterial density, at the same catalyst availability, the threshold needed for cell inactivation is thus reached after a longer period of time. In order to test the reproducibility of the entire process from coating to inactivation, two different fresh discs were tested for *E. coli* inactivation at lower initial cell density. The results (Figure 6, series B1 and B2) show identical inactivation profiles demonstrating the reproducibility of the method of coating and use. A dark control, i.e., a measurement of inactivation with the coated disc without UV irradiation produced no inactivation after 120 min and less than 1 log unit after 210 min. This confirms that the activity in the coated form is via photocatalysis.

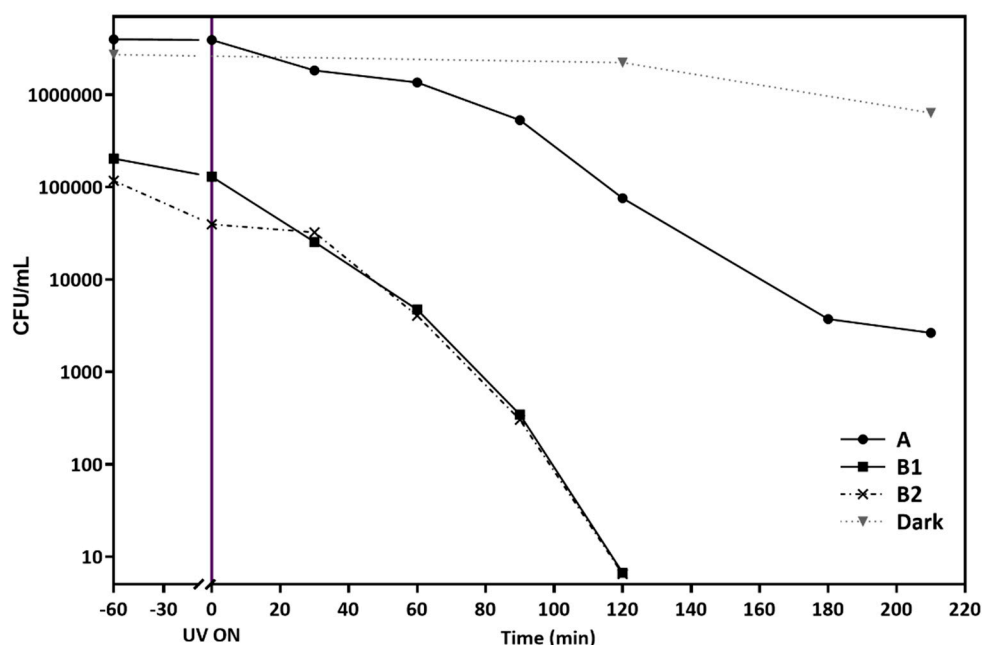


**Figure 6.** Inactivation of *E. coli* starting from  $10^6$  CFU/mL (A) and  $10^5$  CFU/mL (B1 and B2) as well as dark control; all in 1 L and  $380\text{ cm}^2$  Ce-ZnO-coated discs with 38 W UVA.

Rigorous comparisons with literature are not possible due to the fact that UV intensities, bacterial loads and other conditions vary widely. Keeping these differences in mind, comparing immobilised catalysts from literature is still useful in elucidating promising steps for application. Guz et al. [23] used ZnO nanorods immobilised on polyethylene terephthalate and a 300 W UVA lamp (cf. 36 W used herein) and a bacterial density of  $10^8$  CFU/mL in 50 mL of water. Under these conditions, a reduction of 7 log units was reported after 90 min. Since the work herein aims to be a proof of concept, the UVA intensity was not optimised for maximum inactivation but was chosen to evaluate the differences in catalyst activity. Guz et al. [23] work suggests that the UV intensity in this study (from the two 36 W lamps) is nowhere close to saturation for activity and technology upscale should find the best economic balance between the residence time in the reactor and UV power usage. Makwana et al. [49] synthesised  $\text{TiO}_2$  wafers and  $\text{TiO}_2\text{-WO}_3$  composites for the inactivation of *E. coli* in 60 mL of isotonic saline solution using a 75 W xenon lamp. Keeping in mind that the light intensity is higher and the

volume of water is much lower (60 mL), their results are highly encouraging as 4 log units of bacteria were inactivated within 25–30 min.

#### 2.4. Photocatalytic Wastewater Disinfection

The effectiveness of immobilised Ce-ZnO photocatalytic reactor in real wastewater disinfection was also investigated. In particular, the effect on autochthonous bacteria, specifically on antibiotic resistant coliforms and *P. aeruginosa*, and possible enrichment of resistance prevalence (i.e., the change of the ratio of resistant bacteria over total bacteria) were evaluated. This assessment was benchmarked against the TiO<sub>2</sub>-P25 standard photocatalyst immobilised as previously explained. WW1 and WW2 correspond to wastewater samples collected at different times. Aiming at adequate control measurements, the comparison of the performance of Ce-ZnO and TiO<sub>2</sub>-P25 catalysts was studied using different aliquots of the same wastewater sample identified in figures as WW2.

Ce-ZnO was effective at inactivating indigenous *E. coli*, other coliforms and *P. aeruginosa*, as presumptively identified on the respective selective and differential culture media. In all assays, *E. coli* and other coliforms reached lower abundance and were inactivated faster than presumptive *P. aeruginosa* (Figures 7 and 8). In the best case, using Ce-ZnO and WW2, the load of *E. coli* was below the LOQ (0.5 CFU/mL) after 180 min, other coliforms in the same experimental run were at higher levels throughout.

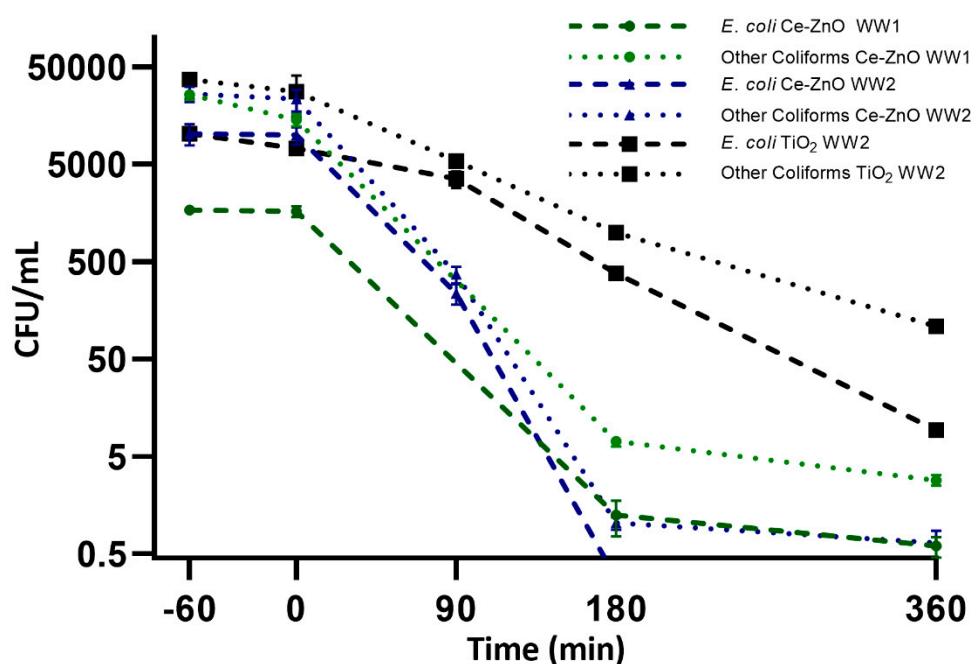


**Figure 7.** Inactivation of *E. coli* and other coliforms Conditions: 750 mL of WW and 380 cm<sup>2</sup> photocatalyst coated discs with 36 W UVA.

In the HPC assays using immobilised titania disc, inactivation of autochthonous was orders of magnitude lower than with the Ce-ZnO disc when the same wastewater (WW2) was used (Figures 7 and 8). These results are consistent with those achieved for the antibiotics (Figure 3), where removal was considerably slower with titania than with Ce-ZnO. The higher activity of Ce-ZnO could be expected considering the results obtained with the antibiotics. Photocatalysts that are more efficient in generating ROS (including HO<sup>•</sup>) will be more effective on treating both chemical species (such as the antibiotics) and biological structures (such as bacterial cell walls) [50]. However, the orders of magnitude differences are not explained simply by the generation of a higher number of radicals because the removal of both antibiotics was not faster to the same extent. The removal of bacteria may be faster with Ce-ZnO because Ce<sup>3+</sup> is inserted in the lattice of ZnO replacing a Zn<sup>2+</sup> ion, thus resulting

in a positively-charged surface that attracts Gram-negative bacterial cell walls, which are generally negatively charged [51].

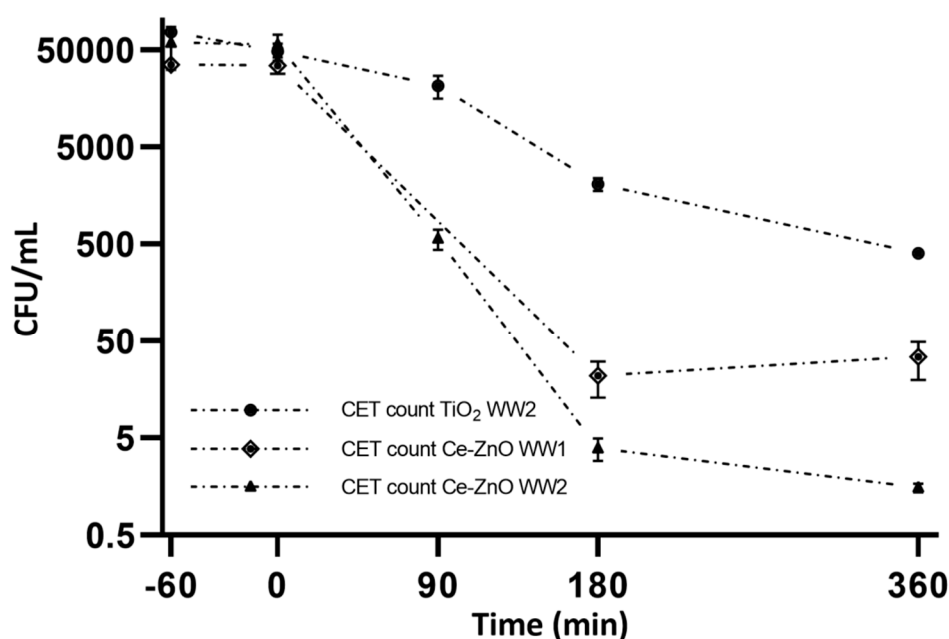
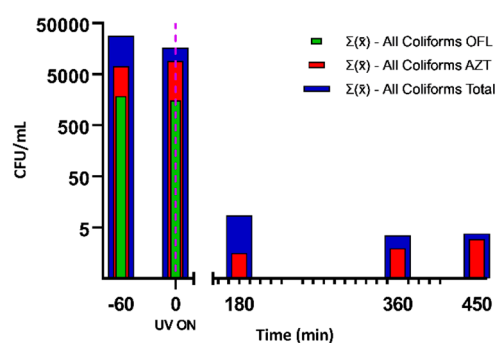


**Figure 8.** Inactivation of *P. aeruginosa*. Conditions: 750 mL of WW and 380 cm<sup>2</sup> photocatalyst coated discs with 36 W UVA.

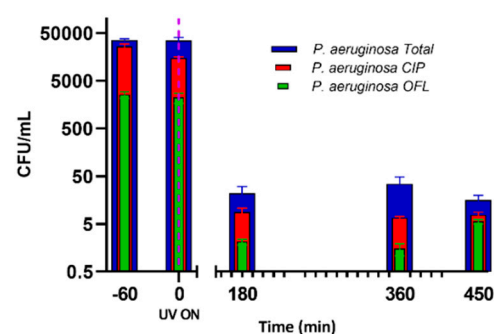
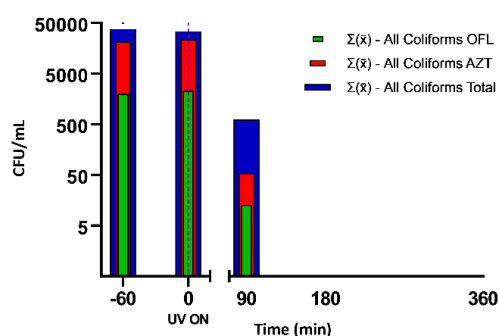
Adán et al. [21] immobilised TiO<sub>2</sub>-P25 on glass rings and used it for the inactivation of *E. coli* and a genus of amoebae in distilled water and synthetic wastewater. As expected, and as the results demonstrated, the inactivation of the bacteria in distilled water was faster than that in wastewater. This can be explained due to presence of other species in the wastewater competing with the pollutants of interest in this study.

In parallel to the determination of the inactivation of bacteria by photocatalysis, the inactivation of the antibiotic resistant fraction of their respective populations was measured using cultivation methods. All the analysed groups were partially inactivated after 180 min exposure.

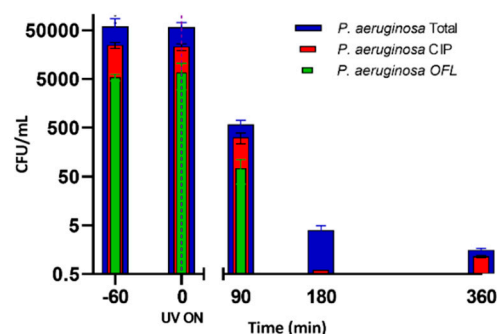
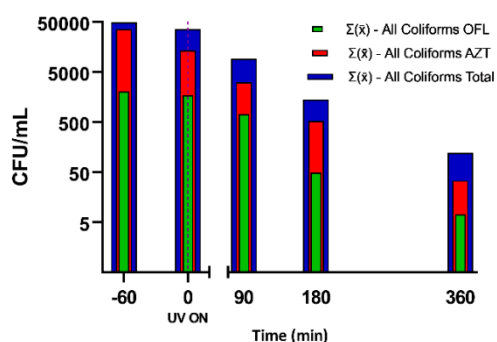
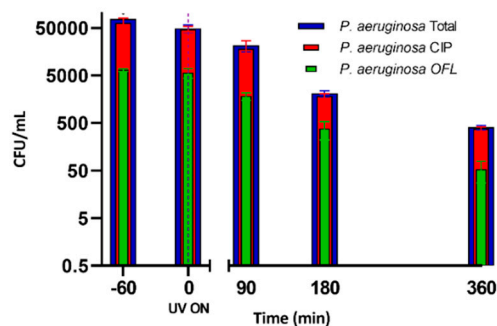
The treatment with both photocatalysts was efficient on the susceptible and resistant fractions of the populations. Ofloxacin resistant coliforms (Figure 9a,c) were below the limit of quantification by 180 min with Ce-ZnO but not with the titania-based disc (Figure 9e). As the effect on *P. aeruginosa* is of concern, the Ce-ZnO photocatalytic process did not substantially affect bacterial loads after 180 min of treatment in WW1 (Figure 9b) and the same was observed for WW2 (Figure 9d) after 90 min, longer treatment times resulting in very low densities of the resistant fractions. Possibly, at lower bacterial densities, other competing species severely outnumbered bacterial biomass and, thus, acted as quenchers for the reaction, resulting in the repair mechanisms of these bacteria outpacing the rate of damage [52]. A higher UV intensity, i.e., one that would be more realistic in real conditions, could potentially overcome this issue. Other options include increasing the coated surface area in contact with water or adding an additional oxidant to kill off the remaining low levels of bacteria.



9a – WW1 Ce-ZnO: coliform count

9b – WW1 Ce-ZnO: *P. aeruginosa* count

9c – WW2 Ce-ZnO: coliform count

9d – WW2 Ce-ZnO: *P. aeruginosa* count9e – WW2 TiO<sub>2</sub>: coliform count9f – WW2 TiO<sub>2</sub>: *P. aeruginosa* count

**Figure 9.** The inactivation of bacteria and their resistant fractions. Inactivation by Ce-ZnO on the sum of *E. coli* and other coliforms in WW1 (9a) and WW2 (9c) and on *P. aeruginosa* in WW1 (9b) and WW2 (9d). The effect of TiO<sub>2</sub>-P25 on the sum of *E. coli* and coliforms in WW2 (9e) and on *P. aeruginosa* in WW2 (9f). Conditions: 750 mL of WW and 380 cm<sup>2</sup> photocatalyst coated discs with 36 W UVA.

It is noteworthy that despite the lower quantity of total and antibiotic resistant *P. aeruginosa* after Ce-ZnO photocatalytic treatment compared to that using TiO<sub>2</sub>, OFL resistant *P. aeruginosa* increased in prevalence between 360 min and 450 min (Figure 9b). This was not observed with TiO<sub>2</sub> possibly due to the fact that at the same conditions titania was slower at inactivating bacteria and did not reach the low bacterial loads reached with Ce-ZnO. In the experiments conducted with TiO<sub>2</sub> and Ce-ZnO as catalysts, and using the same wastewater to compare the efficiency of these catalysts, Ce-ZnO gave lower ranges of prevalence of resistance for *E. coli* and other coliforms after 90 min (Table 2). As for titania, the changes are less drastic after 90 min of photocatalytic treatment.

**Table 2.** Resistant fractions  $\pm$  SD after 90 min of treatment with Ce-ZnO and TiO<sub>2</sub>.

Exp		Initial (t = -60)			After 90 min Treatment		
		OFL Resistant %	AZT Resistant %	CIP Resistant %	OFL Resistant %	AZT Resistant %	CIP Resistant %
Ce ZnO	<i>E. coli</i>	7.0–11.5	56.0–67.1	N/A	2.1–2.8	2.9–8.0	N/A
	Other Coliforms	3.6–4.6	53.4–56.7	N/A	1.5–2.2	9.8–10.9	N/A
	<i>P. aeruginosa</i>	7.2–14.6	N/A	32.7–67.9	7.9–15.9	N/A	52.8–55.4
TiO <sub>2</sub>	<i>E. coli</i>	8.7–8.8	55.7–74.2	N/A	8.6–9.7	5.6–15.7	N/A
	Other Coliforms	1.6–4.0	75.0–78.0	N/A	4.0–9.1	43.7–53.1	N/A
	<i>P. aeruginosa</i>	8.5–8.6	N/A	62.8–99.5	8.0–9.6	N/A	56.3–99.5

### 3. Materials and Methods

#### 3.1. Wastewater Samples

Wastewater was collected from the secondary clarifier of an UWTP in Northern Portugal. Two wastewater samples were taken and identified as WW1 having a dissolved organic carbon (DOC) of 20.6 mg/L and WW2 with a DOC of 34.6 mg/L. Wastewater UV-VIS absorption spectra are reported as Figure S1 in Supplementary Information (SI), while other monthly parameters as provided by the UWTP manager, are shown in Table 3.

**Table 3.** Monthly averaged and range of physicochemical parameters.

Monthly	Secondary Clarifier					
	pH	Conductivity ( $\mu$ S/Cm)	BOD <sub>5</sub> (mg/L)	COD (mg/L)	TSS (mg/L)	VSS (mg/L)
Average	7.2	707	31.3	90.3	33.5	31.4
Min	7.0	590	15.6	16.0	23.0	22.0
Max	7.5	859	95.3	204.0	76.0	76.0

BOD<sub>5</sub> = five-day biochemical oxygen demand; COD = chemical oxygen demand; TSS = total suspended solids; VSS = volatile suspended solids.

#### 3.2. Photocatalyst Synthesis, Immobilisation and Characterisation

Circular discs made of 304 grade stainless steel were mechanically treated with aluminium oxide sand paper of grit P60 to increase the surface roughness, followed by sonication in acetone for 15 min to remove any surface lubricants from the cutting process. After cleaning and drying, the discs were heated at 400 °C for 1 h to induce a slight surface oxidation.

Following mechanical treatment, a silica interlayer was deposited on the discs. A two-step procedure proposed by Schaefer and Keefer [53] was used. Tetraethyl orthosilicate (TEOS), propan-2-ol and water were mixed together in a 1:3:1 mole ratio and heated to 60 °C. A volume corresponding to 0.7 millimoles of hydrochloric acid (HCl) was added per mole of water and the mixture left stirring for 1.5 h at 60 °C. After 1.5 hrs of stirring, 11 mole parts of water and 0.0043 mole parts of HCl, giving a pH of 2–3, were added and left stirring overnight. The mixture was then sprayed directly on a warmed disc multiple times, with intervals to allow evaporation of the mixture. After drying, the discs were calcined at 400 °C for 1 h with a ramp of 2 °C/min and passive cooling.

Ce-ZnO at 0.04:1 Ce:Zn atom-to atom ratio was prepared via the hydroxide induced hydrolysis method, as previously published [26]. Briefly, 16.8 millimoles of zinc nitrate (Sigma Aldrich, St. Louis MI, USA, >99% purum) and 0.67 millimoles of cerium (III) nitrate (Alfa Aesar, Haverhill, MA, USA, 99.5%) were dissolved in 75 mL of water under stirring. Separately, 55 millimoles of sodium hydroxide (JMGS LDA) were dissolved in 25 mL of water. Under vigorous stirring, the basic solution was added dropwise to the aqueous mixture of Ce(III) and Zn(II) salts. The hydroxide precipitate was centrifuged at 5000  $\times$  g for 5 min and washed twice with 100 mL of water. Coating was carried out by re-suspending the hydroxide precipitate that was formed under sonication for 5 min, and aerosol sprayed directly on

a warmed disc previously coated with the silica interlayer and then calcined at 300 °C for 1 h with a ramp of 2 °C/min and passive cooling, giving a white coat of cerium-doped ZnO.

For comparison, discs were also coated with undoped ZnO and TiO<sub>2</sub>-P25, the latter being the standard photocatalyst in the literature. The pre-treatment and interlayer coating were identical to the coating procedure used for Ce-ZnO. The only difference was that no cerium salt was added prior to hydroxide precipitation when preparing undoped ZnO. In the case of TiO<sub>2</sub>-P25, it was sprayed directly onto the disc from a 1% TiO<sub>2</sub>-P25 aqueous suspension, followed by the same thermal treatment.

The silica interlayer as well as the Ce-ZnO coatings were characterised directly on stainless steel, by X-ray diffraction (XRD) analysis carried out on Bruker D8 diffractometer, with a scan rate equal to 0.05 °/s.

### 3.3. Photocatalytic Experiments

The photocatalytic degradation of SMX and TMP in pure water was studied using three immobilised catalysts (i.e., Ce-ZnO, undoped ZnO and TiO<sub>2</sub>-P25). For antibiotic removal, each catalyst was immobilised on 11.5 cm diameter (area = 104 cm<sup>2</sup>) discs. Both antibiotics were at >98% purity and purchased from Sigma-Aldrich. A stock solution at 0.25 mM of each antibiotic in methanol was prepared and stored at 4 °C protected from light. Prior to each experiment, the stock solution was warmed to room temperature and homogenised. A volume of 1 mL of stock solution was accurately pipetted to a 1 L volumetric flask. Methanol was removed with a gentle flow of dry nitrogen gas until all of the liquid evaporated. Then, the volumetric flask was filled up with 1 L of Milli-Q water and sonicated to re-dissolve the antibiotics. The final concentration of each antibiotic was 0.25 μM (SMX = 6.332 μg/L and TMP = 7.258 μg/L). The pH values of SMX and TMP aqueous solutions were 6.28 and 6.19, respectively; the pH of the mixture (TMP + SMX) being 6.22. The aqueous solution of antibiotics was then placed in a round borosilicate glass container with a diameter of 18 cm and a water height of 4 cm, which was magnetically stirred and surrounded by an external water jacket to maintain the reaction temperature at about 25 °C. Each experimental test involved a 60 min dark phase for adsorption equilibrium to be reached. Following this, UVA irradiation was supplied from a distance of 10 cm from the base by two Osram Dulux®L BL UVA 18W/78 (spectrum in Figure S2) with an Osram Quicktronic Professional®Optimal QTP-OPTIMAL 2X18-40 ballast. A low UVA intensity was used to allow for a more gradual decay of analytes which makes it easier to elucidate differences between the tested catalysts.

The coating efficacy and stability of the Ce-ZnO disc was also tested by reusing the same Ce-ZnO disc for five times without chemical regeneration. The disc was only dried at 80 °C for about 0.5 h between each reuse cycle.

Separately, the applicability of the immobilised Ce-ZnO catalyst in the photocatalytic inactivation of *Escherichia coli* (DH5-Alpha kindly supplied by C. Merlin LCPM/Université de Lorraine CNRS) in isotonic sodium chloride solution was also investigated. The light source was identical but a larger 22 cm diameter (area = 380 cm<sup>2</sup>) 304 stainless steel disc, coated as previously detailed, was used for inactivation experiments, using 1 L of 0.85% NaCl in a 260 mm diameter container with overhead stirring and external circulating water bath for thermoregulation.

Fresh LB agar cultures of *E. coli* were suspended in saline solution to reach an optical density of 1.0 at 610 nm. A total of three inactivation experiments were carried out, two with an initial cell density of 10<sup>5</sup> CFU/mL (spiking 0.1 mL of 1.0 OD<sub>610</sub> stock) and another with an initial density of 10<sup>6</sup> CFU/mL (spiking 1.0 mL of 1.0 OD<sub>610</sub> stock).

Disinfection photocatalytic tests with secondary treated wastewater were performed through previously unused stainless-steel discs with immobilised Ce-ZnO and TiO<sub>2</sub>-P25. Due to the high UVA absorption of the wastewaters to be disinfected (Figure S1), a lower water volume (750 mL) was used in these disinfection experiments, to reduce the water depth and hence the absorption of UVA by the column of wastewater between the light source and the immobilised catalyst.

### 3.4. Bacterial Count

For experimental assays with spiked *E. coli*, colonies were enumerated on plate count agar (PCA, Merck, Darmstadt, Germany) incubated for 24 h at 37 °C. For experiments with real wastewater, autochthonous bacteria were also enumerated to putatively assess the prevalence of AR, as previously described in the scientific literature [54–58]. Two selective media were used, the Chromogenic Coliform Agar (referred to as CCA) for quantification of *E. coli* and other coliforms; and 0.3% Cetrimide Agar (referred to as CET) with 15 µg/mL of nalidixic acid for quantification of *Pseudomonas aeruginosa* [59]. For CCA, plates with two antibiotics, ofloxacin (8 µg/mL) or azithromycin (32 µg/mL) were used. For CET again two antibiotics were used, ofloxacin (8 µg/mL) or ciprofloxacin (1 µg/mL). The concentrations of antibiotics for CCA were as per CLSI guidelines for *Enterobacteriaceae* [60]. For CET, antibiotic concentrations of ofloxacin were again as per CLSI guidelines for *Pseudomonas aeruginosa* while for ciprofloxacin a more environmentally relevant cut-off concentration (1 µg/mL) for resistance, which also has been previously reported, was chosen instead [61,62]. Resistance was estimated based on the ratio of the number of colonies enumerated in the presence of an antibiotic to the enumeration in its absence, using the equation below:

$$\text{resistance fraction of bacterial population} = \frac{\text{colonies on antibiotic spiked agar}}{\text{colonies on agar without antibiotic}} \quad (1)$$

Enumeration of the bacteria in wastewater was performed by the membrane filtration method, using 0.45 µm membranes and incubating at 37 °C for 24 h. *E. coli* and other coliforms were differentiated by the colour of the colonies (blue for *E. coli* and pink for other coliforms) grown on CCA as per manufacturer's instructions.

### 3.5. Analytical Measurements

Antibiotic degradation was analysed in triplicate using an ultra-high performance liquid chromatography with tandem Mass Spectrometry (UHPLC-MS/MS), using a Shimadzu Corporation apparatus (Kyoto, Japan) consisting of a Nexera UHPLC equipment coupled to a triple quadrupole mass spectrometer (Ultra Fast Mass Spectrometry series LCMS-8040), with an ESI source operating in both positive and negative ionisation modes. A Kinetex™ 1.7 µm XB-C18 100 Å column (100 × 2.1 mm i.d.) (Phenomenex, Inc., Torrance, CA, USA) was employed for chromatographic separation under isocratic mode, using a mixture (1:4, *v/v*) of an aqueous solution of 0.1% formic acid (Fisher Scientific, Loughborough, UK) and a solution of methanol and acetonitrile (1:1, *v/v*) (both MS grade VWR International Fontenay-sous-Bois, France), at a flow rate of 0.20 mL/min.

Column oven and autosampler temperatures were set at 35 °C and 4 °C, respectively. The injection volume was 10 µL. Selected reaction monitoring (SRM) was performed for analysis, evaluating the two SRM transitions between the precursor ion and the two most abundant fragment ions for each compound, with a scan time of 100 ms per transition, being the SRM between the precursor ion and the most abundant fragment ion used for quantification and the second most abundant for confirmation purposes (Table S1). The collision induced dissociation gas (CID) was argon at 230 kPa. The drying gas and nebulizing gas flows, capillary voltage, desolvation and source temperatures were respectively: 15 L/min, 3.0 L/min; 4.5 kV, 400 °C and 250 °C. Removal values were expressed as ratios of the area after 60 min of dark phase over area at time of sampling.

DOC measurements were conducted using a Shimadzu TOC-L analyser, after filtering the samples.

## 4. Conclusions

A simple and low-cost method was used to synthesise cerium-doped zinc oxide (Ce-ZnO) and immobilise it on ordinary 304 stainless steel discs by aerosol spraying of the hydroxide precursor suspension on the pre-treated metal. The comparison of Ce-ZnO, undoped ZnO and the benchmarking standard TiO<sub>2</sub>-P25 photocatalyst for the degradation of two selected antibiotics (SMX and TMP)

showed that the slowest removal rate is obtained with TiO<sub>2</sub>-P25, while Ce-ZnO was the most active at removing SMX and undoped ZnO more active at removing TMP. The immobilised catalyst was easy to reuse and a Ce-ZnO coated disc was used in five consecutive runs. The system was also tested against spiked *E. coli* in isotonic saline solution where it was also active, differently coated discs revealing consistent inactivation kinetics, reinforcing the robustness of the facile coating procedure. Dark controls gave only negligible inactivation. Finally, the immobilised Ce-ZnO catalyst was used for the disinfection of real secondary treated wastewater, including the inactivation of antibiotic-resistant bacteria, and a direct comparison with immobilised TiO<sub>2</sub>-P25 was also performed. Ce-ZnO was around two-orders of magnitude faster than TiO<sub>2</sub>-P25 in the inactivation of indigenous bacteria. With short reaction times, no evidence for enrichment of resistance was observed. However, with extended reaction times, low levels of bacterial loads were not further inactivated, suggesting that a higher UV intensity or an additional oxidant is required to reach even lower levels of bacterial density.

**Supplementary Materials:** The following are available online at <http://www.mdpi.com/2073-4344/9/3/222/s1>, Figure S1. Absorbance spectra of wastewater samples (WW1 and WW2) used for disinfection experiments, using a 1 cm cell. Figure S2. Relative Intensity Spectrum of Osram UVA 18W/78 CFL. Table S1. Chemical structure, M<sub>w</sub>, pK<sub>a</sub> and selected reaction monitoring (SRM) transitions between the precursor ion and the two most abundant fragment ions for each antibiotic.

**Author Contributions:** Funding acquisition: C.M.M. and L.R.; investigation: I.Z.; methodology: A.R.R. (LC-MS analyses); resources: A.M.T.S. and C.M.M.; supervision: V.V., A.M.T.S., C.M.M., and L.R.; visualization: I.Z.; writing—original draft: I.Z. writing—review and editing: V.V., A.R.R., A.M.T.S., C.M.M., and L.R.

**Funding:** This work is part of a project that has received funding from the European Union's Horizon 2020, under the Innovative Training Networks (ITN-ETN) programme Marie Skłodowska-Curie grant (ANTibioticS and mobile resistance elements in WastEwater Reuse applications: risks and innovative solutions) agreement no. 675530. The authors would also like to acknowledge the financial support provided by COST-European Cooperation in Science and Technology, to the COST Action ES1403: New and emerging challenges and opportunities in wastewater reuse (NEREUS). The content herein reflects only the authors' views and the Research Executive Agency and neither COST nor any person acting on its behalf is responsible for any use that may be made of the information it contains. Additionally, this work was partially supported by: Associate Laboratory LSRE-LCM—UID/EQU/50020/2019—funded by national funds through FCT/MCTES (PIDDAC).

**Acknowledgments:** Telma Fernandes, Iakovos Iakovides, Francesco Biancillo, Nuno F.F. Moreira and Ivone Vaz-Moreira are acknowledged for their help and advice at the lab. Anabela Nogueira and Sérgio C. Silva from Adventech Lda. are acknowledged for offering equipment and logistical support.

**Conflicts of Interest:** The authors declare no conflict of interest. The funders had no role in the design of the study; in the collection, analyses, or interpretation of data; in the writing of the manuscript, or in the decision to publish the results

## References

1. O'Neill, J. Tackling Drug-Resistant Infections Globally: Final Report and Recommendations. 2016. Available online: [https://amr-review.org/sites/default/files/160518\\_Final%20paper\\_with%20cover.pdf](https://amr-review.org/sites/default/files/160518_Final%20paper_with%20cover.pdf) (accessed on 14 February 2019).
2. Rizzo, L.; Manaia, C.; Merlin, C.; Schwartz, T.; Dagot, C.; Ploy, M.; Michael, I.; Fatta-Kassinos, D. Urban wastewater treatment plants as hotspots for antibiotic-resistant bacteria and genes spread into the environment: A review. *Sci. Total Environ.* **2013**, *447*, 345–360. [CrossRef] [PubMed]
3. Larsson, D.J.; Andremon, A.; Bengtsson-Palme, J.; Brandt, K.K.; Husman, A.M.D.R.; Fagerstedt, P.; Fick, J.; Flach, C.-F.; Gaze, W.H.; Kuroda, M.; et al. Critical knowledge gaps and research needs related to the environmental dimensions of antibiotic resistance. *Environ. Int.* **2018**, *117*, 132–138. [CrossRef] [PubMed]
4. Berendonk, T.U.; Manaia, C.M.; Merlin, C.; Fatta-Kassinos, D.; Cytryn, E.; Walsh, F.; Bürgmann, H.; Sørum, H.; Norström, M.; Pons, M.-N.; et al. Tackling antibiotic resistance: The environmental framework. *Nat. Rev. Microbiol.* **2015**, *13*, 310–317. [CrossRef] [PubMed]
5. Manaia, C.M.; Rocha, J.; Scaccia, N.; Marano, R.; Radu, E.; Biancillo, F.; Cerqueira, F.; Fortunato, G.; Iakovides, I.C.; Zammit, I.; et al. Antibiotic resistance in wastewater treatment plants: Tackling the black box. *Environ. Int.* **2018**, *115*, 312–324. [CrossRef] [PubMed]
6. Wright, G.D. Antibiotic resistance in the environment: A link to the clinic? *Curr. Opin. Microbiol.* **2010**, *13*, 589–594. [CrossRef] [PubMed]

7. Bates, B.; Kundzewicz, Z.; Wu, S.; Palutikof, J. *Climate Change and Water Technical Paper of the Intergovernmental Panel on Climate Change*; IPCC Secretariat: Geneva, Switzerland, 2008; Volume 95, p. 96. Available online: [https://digital.library.unt.edu/ark:/67531/metadc11958/m2/1/high\\_res\\_d/climate-change-water-en.pdf](https://digital.library.unt.edu/ark:/67531/metadc11958/m2/1/high_res_d/climate-change-water-en.pdf) (accessed on 14 February 2019).
8. BIO by Deloitte. *Optimising Water Reuse in the EU—Final Report Prepared for the European Commission (DG ENV) Part 1*. 07.0307/2013/658572/ENV.C1. 2015. Available online: [http://ec.europa.eu/environment/water/blueprint/pdf/BIO\\_IA%20on%20water%20reuse\\_Final%20Part%20I.pdf](http://ec.europa.eu/environment/water/blueprint/pdf/BIO_IA%20on%20water%20reuse_Final%20Part%20I.pdf) (accessed on 14 February 2019).
9. Rizzo, L.; Krätke, R.; Linders, J.; Scott, M.; Vighi, M.; De Voogt, P. Proposed EU minimum quality requirements for water reuse in agricultural irrigation and aquifer recharge: SCHEER scientific advice. *Curr. Opin. Environ. Sci. Health* **2018**, *2*, 7–11. [[CrossRef](#)]
10. Murray, G.E.; Tobin, R.S.; Junkins, B.; Kushner, D.J. Effect of chlorination on antibiotic resistance profiles of sewage-related bacteria. *Appl. Environ. Microbiol.* **1984**, *48*, 73–77. [[PubMed](#)]
11. Liu, S.-S.; Qu, H.-M.; Yang, D.; Hu, H.; Liu, W.-L.; Qiu, Z.-G.; Hou, A.-M.; Guo, J.; Li, J.-W.; Shen, Z.-Q.; et al. Chlorine disinfection increases both intracellular and extracellular antibiotic resistance genes in a full-scale wastewater treatment plant. *Water Res.* **2018**, *136*, 131–136. [[CrossRef](#)] [[PubMed](#)]
12. Zheng, J.; Su, C.; Zhou, J.; Xu, L.; Qian, Y.; Chen, H. Effects and mechanisms of ultraviolet, chlorination, and ozone disinfection on antibiotic resistance genes in secondary effluents of municipal wastewater treatment plants. *Biochem. Eng. J.* **2017**, *317*, 309–316. [[CrossRef](#)]
13. Alexander, J.; Knopp, G.; Dötsch, A.; Wieland, A.; Schwartz, T. Ozone treatment of conditioned wastewater selects antibiotic resistance genes, opportunistic bacteria, and induce strong population shifts. *Sci. Total Environ.* **2016**, *559*, 103–112. [[CrossRef](#)] [[PubMed](#)]
14. Rizzo, L.; Della Sala, A.; Fiorentino, A.; Puma, G.L. Disinfection of urban wastewater by solar driven and UV lamp–TiO<sub>2</sub> photocatalysis: Effect on a multi drug resistant *Escherichia coli* strain. *Water Res.* **2014**, *53*, 145–152. [[CrossRef](#)] [[PubMed](#)]
15. Sacco, O.; Vaiano, V.; Rizzo, L.; Sannino, D. Photocatalytic activity of a visible light active structured photocatalyst developed for municipal wastewater treatment. *J. Clean. Prod.* **2018**, *175*, 38–49. [[CrossRef](#)]
16. Richardson, S.D.; Plewa, M.J.; Wagner, E.D.; Schoeny, R.; DeMarini, D.M. Occurrence, genotoxicity, and carcinogenicity of regulated and emerging disinfection by-products in drinking water: A review and roadmap for research. *Mut. Res.-Rev. Mut. Res.* **2007**, *636*, 178–242. [[CrossRef](#)] [[PubMed](#)]
17. Wildhaber, Y.S.; Mestankova, H.; Schärer, M.; Schirmer, K.; Salhi, E.; Von Gunten, U. Novel test procedure to evaluate the treatability of wastewater with ozone. *Water Res.* **2015**, *75*, 324–335. [[CrossRef](#)] [[PubMed](#)]
18. Rizzo, L.; Malato, S.; Antakyali, D.; Beretsou, V.G.; Đolić, M.B.; Gernjak, W.; Heath, E.; Ivancev-Tumbas, I.; Karaolia, P.; Lado Ribeiro, A.R.; et al. Consolidated vs. new advanced treatment methods for the removal of contaminants of emerging concern from urban wastewater. *Sci. Total Environ.* **2019**, *655*, 986–1008. [[CrossRef](#)] [[PubMed](#)]
19. Van Grieken, R.; Marugan, J.; Sordo, C.; Martínez, P.; Pablos, C. Photocatalytic inactivation of bacteria in water using suspended and immobilized silver-TiO<sub>2</sub>. *Appl. Catal. B-Environ.* **2009**, *93*, 112–118. [[CrossRef](#)]
20. Alrousan, D.M.; Dunlop, P.S.; McMurray, T.A.; Byrne, J.A. Photocatalytic inactivation of *E. coli* in surface water using immobilised nanoparticle TiO<sub>2</sub> films. *Water Res.* **2009**, *43*, 47–54. [[CrossRef](#)] [[PubMed](#)]
21. Adán, C.; Magnet, A.; Fenoy, S.; Pablos, C.; Del Águila, C.; Marugán, J. Concomitant inactivation of *Acanthamoeba* spp. and *Escherichia coli* using suspended and immobilized TiO<sub>2</sub>. *Water Res.* **2018**, *144*, 512–521. [[CrossRef](#)] [[PubMed](#)]
22. Pablos, C.; Van Grieken, R.; Marugan, J.; Moreno, B.; Moreno-García, B. Photocatalytic inactivation of bacteria in a fixed-bed reactor: Mechanistic insights by epifluorescence microscopy. *Catal. Today* **2011**, *161*, 133–139. [[CrossRef](#)]
23. Guz, L.; García, P.; Ponce, S.; Goyanes, S.; Marchi, M.C.; Candal, R.; Rodríguez, J.; Sanchez, L. Synthesis and Characterization of ZnO Nanorod Films on PET for Photocatalytic Disinfection of Water. *J. Adv. Oxid. Tech.* **2015**, *18*, 246–252.
24. Yeber, M.C.; Rodríguez, J.; Freer, J.; Durán, N.; Mansilla, H.D. Photocatalytic degradation of cellulose bleaching effluent by supported TiO<sub>2</sub> and ZnO. *Chemosphere* **2000**, *41*, 1193–1197. [[CrossRef](#)]
25. Couto, S.R.; Domínguez, A.; Sanromán, A. Photocatalytic degradation of dyes in aqueous solution operating in a fluidised bed reactor. *Chemosphere* **2002**, *46*, 83–86. [[CrossRef](#)]

26. Zammit, I.; Vaiano, V.; Iervolino, G.; Rizzo, L. Inactivation of an urban wastewater indigenous *Escherichia coli* strain by cerium-doped zinc oxide photocatalysis. *RSC Adv.* **2018**, *8*, 26124–26132. [[CrossRef](#)]
27. Krzeminski, P.; Tomei, M.C.; Karaolia, P.; Langenhoff, A.; Almeida, C.M.R.; Felis, E.; Gritten, F.; Andersen, H.R.; Fernandes, T.; Manaia, C.M.; et al. Performance of secondary wastewater treatment methods for the removal of contaminants of emerging concern implicated in crop uptake and antibiotic resistance spread: A review. *Sci. Total Environ.* **2019**, *648*, 1052–1081. [[CrossRef](#)] [[PubMed](#)]
28. Fernández, A.; Lassaletta, G.; Jiménez, V.; Justo, A.; González-Elipe, A.; Herrmann, J.-M.; Tahiri, H.; Ait-Ichou, Y. Preparation and characterization of TiO<sub>2</sub> photocatalysts supported on various rigid supports (glass, quartz and stainless steel). Comparative studies of photocatalytic activity in water purification. *Appl. Catal. B-Environ.* **1995**, *7*, 49–63. [[CrossRef](#)]
29. Cheary, R.W.; Ma-Sorrell, Y. Quantitative phase analysis by X-ray diffraction of martensite and austenite in strongly oriented orthodontic stainless steel wires. *J. Mater. Sci.* **2000**, *35*, 1105–1113. [[CrossRef](#)]
30. Fathi, M.; Karimzadeh, F.; Dadfar, M.; Saatchi, A. Effect of TIG welding on corrosion behavior of 316L stainless steel. *Mat. Lett.* **2007**, *61*, 2343–2346.
31. Boreen, A.L.; Arnold, W.A.; McNeill, K. Photochemical Fate of Sulfa Drugs in the Aquatic Environment: Sulfa Drugs Containing Five-Membered Heterocyclic Groups. *Environ. Sci. Technol.* **2004**, *38*, 3933–3940. [[CrossRef](#)] [[PubMed](#)]
32. Dodd, M.C.; Buffle, M.-O.; Von Gunten, U. Oxidation of Antibacterial Molecules by Aqueous Ozone: Moiety-Specific Reaction Kinetics and Application to Ozone-Based Wastewater Treatment. *Environ. Sci. Technol.* **2006**, *40*, 1969–1977. [[CrossRef](#)] [[PubMed](#)]
33. Dionysiou, D.D.; Puma, G.L.; Ye, J.; Schneider, J.; Bahnemann, D. *Photocatalysis: Applications*; The Royal Society of Chemistry: Cambridge, UK, 2016.
34. Zhang, L.; Cheng, H.; Zong, R.; Zhu, Y. Photocorrosion Suppression of ZnO Nanoparticles via Hybridization with Graphite-like Carbon and Enhanced Photocatalytic Activity. *J. Phys. Chem. C* **2009**, *113*, 2368–2374. [[CrossRef](#)]
35. Pekakis, P.A.; Xekoukoulotakis, N.P.; Mantzavinos, D. Treatment of textile dyehouse wastewater by TiO<sub>2</sub> photocatalysis. *Water Res.* **2006**, *40*, 1276–1286. [[CrossRef](#)] [[PubMed](#)]
36. Rao, A.N.; Sivasankar, B.; Sadasivam, V. Kinetic study on the photocatalytic degradation of salicylic acid using ZnO catalyst. *J. Hazard. Mater.* **2009**, *166*, 1357–1361. [[PubMed](#)]
37. Fernandez-Ibanez, P.; Blanco, J.; Malato, S.; Nieves, F.L. Application of the colloidal stability of TiO<sub>2</sub> particles for recovery and reuse in solar photocatalysis. *Water Res.* **2003**, *37*, 3180–3188. [[CrossRef](#)]
38. Chakrabarti, S.; Dutta, B. Photocatalytic degradation of model textile dyes in wastewater using ZnO as semiconductor catalyst. *J. Hazard. Mater.* **2004**, *112*, 269–278. [[CrossRef](#)] [[PubMed](#)]
39. Hong, Y.; Tian, C.; Jiang, B.; Wu, A.; Zhang, Q.; Tian, G.; Fu, H. Facile synthesis of sheet-like ZnO assembly composed of small ZnO particles for highly efficient photocatalysis. *J. Mater. Chem. A* **2013**, *1*, 5700–5708. [[CrossRef](#)]
40. Rimoldi, L.; Meroni, D.; Cappelletti, G.; Ardizzone, S. Green and low cost tetracycline degradation processes by nanometric and immobilized TiO<sub>2</sub> systems. *Catal. Today* **2017**, *281*, 38–44. [[CrossRef](#)]
41. Pronina, N.; Klauson, D.; Moiseev, A.; Deubener, J.; Krichevskaya, M. Titanium dioxide sol–gel-coated expanded clay granules for use in photocatalytic fluidized-bed reactor. *Appl. Catal. B-Environ.* **2015**, *178*, 117–123. [[CrossRef](#)]
42. Akhavan, O. Lasting antibacterial activities of Ag–TiO<sub>2</sub>/Ag/a-TiO<sub>2</sub> nanocomposite thin film photocatalysts under solar light irradiation. *J. Colloid Interface Sci.* **2009**, *336*, 117–124. [[CrossRef](#)] [[PubMed](#)]
43. Shan, A.Y.; Ghazi, T.I.M.; Rashid, S.A. Immobilisation of titanium dioxide onto supporting materials in heterogeneous photocatalysis: A review. *Appl. Catal. A Gen.* **2010**, *389*, 1–8. [[CrossRef](#)]
44. Lalhriatpuia, C.; Tiwari, D.; Tiwari, A.; Lee, S.M. Immobilized Nanopillars-TiO<sub>2</sub> in the efficient removal of micro-pollutants from aqueous solutions: Physico-chemical studies. *Biochem. Eng. J.* **2015**, *281*, 782–792.
45. Van Doorslaer, X.; Demeestere, K.; Heynderickx, P.M.; Van Langenhove, H.; Dewulf, J. UV-A and UV-C induced photolytic and photocatalytic degradation of aqueous ciprofloxacin and moxifloxacin: Reaction kinetics and role of adsorption. *Appl. Catal. B-Environ.* **2011**, *101*, 540–547. [[CrossRef](#)]
46. Ozer, L.Y.; Garlisi, C.; Oladipo, H.; Pagliaro, M.; Sharief, S.A.; Yusuf, A.; Almheiri, S.; Palmisano, G. Inorganic semiconductors-graphene composites in photo(electro)catalysis: Synthetic strategies, interaction mechanisms and applications. *J. Photochem. Photobiol. C-Photochem. Rev.* **2017**, *33*, 132–164. [[CrossRef](#)]

47. Sarvari, M.H.; Sharghi, H. Reactions on a Solid Surface. A Simple, Economical and Efficient Friedel–Crafts Acylation Reaction over Zinc Oxide (ZnO) as a New Catalyst. *J. Org. Chem.* **2004**, *69*, 6953–6956. [[CrossRef](#)] [[PubMed](#)]
48. Kiwi, J.; Nadtochenko, V. Evidence for the Mechanism of Photocatalytic Degradation of the Bacterial Wall Membrane at the TiO<sub>2</sub> Interface by ATR-FTIR and Laser Kinetic Spectroscopy. *Langmuir* **2005**, *21*, 4631–4641. [[CrossRef](#)] [[PubMed](#)]
49. Makwana, N.M.; Hazael, R.; McMillan, P.F.; Darr, J.A. Photocatalytic water disinfection by simple and low-cost monolithic and heterojunction ceramic wafers. *Photochem. Photobiol. Sci.* **2015**, *14*, 1190–1196. [[CrossRef](#)] [[PubMed](#)]
50. Cho, M.; Chung, H.; Choi, W.; Yoon, J. Linear correlation between inactivation of *E. coli* and OH radical concentration in TiO<sub>2</sub> photocatalytic disinfection. *Water Res.* **2004**, *38*, 1069–1077. [[CrossRef](#)] [[PubMed](#)]
51. Grijpma, D.W.; Feijen, J.; Busscher, H.J.; Gottenbos, B.; Van Der Mei, H.C. Antimicrobial effects of positively charged surfaces on adhering Gram-positive and Gram-negative bacteria. *J. Antimicrob. Chemother.* **2001**, *48*, 7–13.
52. Das, S.; Sinha, S.; Jayabalan, R.; Suar, M.; Mishra, A.; Tamhankar, A.J.; Tripathy, S.K.; Lundborg, C.S. Disinfection of Multidrug Resistant *Escherichia coli* by Solar-Photocatalysis using Fe-doped ZnO Nanoparticles. *Sci. Rep.* **2017**, *7*, 109. [[CrossRef](#)] [[PubMed](#)]
53. Schaefer, D.W.; Keefer, K.D. Structure of Soluble Silicates. *MRS Proc.* **1984**, *32*. [[CrossRef](#)]
54. Watkinson, A.J.; Micalizzi, G.R.; Bates, J.R.; Costanzo, S.D. Novel Method for Rapid Assessment of Antibiotic Resistance in *Escherichia coli* Isolates from Environmental Waters by Use of a Modified Chromogenic Agar. *Appl. Environ. Microbiol.* **2007**, *73*, 2224–2229. [[CrossRef](#)] [[PubMed](#)]
55. Walter, M.V.; Vennes, J.W. Occurrence of multiple-antibiotic-resistant enteric bacteria in domestic sewage and oxidation lagoons. *Appl. Environ. Microbiol.* **1985**, *50*, 930–933. [[PubMed](#)]
56. Carpa, R.; Oltean, A.; Popescu, O.; Lupan, I.; Kelemen, B.S. Release of Antibiotic-resistant bacteria by a Waste Treatment Plant from Romania. *Microb. Environ.* **2017**, *32*, 219–225.
57. Kim, S.; Jensen, J.; Aga, D.; Weber, A. Fate of tetracycline resistant bacteria as a function of activated sludge process organic loading and growth rate. *Water Sci. Technol.* **2007**, *55*, 291–297. [[CrossRef](#)] [[PubMed](#)]
58. Huang, J.-J.; Hu, H.-Y.; Lu, S.-Q.; Li, Y.; Tang, F.; Lu, Y.; Wei, B. Monitoring and evaluation of antibiotic-resistant bacteria at a municipal wastewater treatment plant in China. *Environ. Int.* **2012**, *42*, 31–36. [[CrossRef](#)] [[PubMed](#)]
59. Goto, S.; Enomoto, S. Nalidixic Acid Cetrime Agar. *Jpn. J. Microbiol.* **1970**, *14*, 65–72. [[CrossRef](#)] [[PubMed](#)]
60. CLSI. *Performance Standards for Antimicrobial Susceptibility Testing*; Twenty-Fifth Informational Supplement; Clinical and Laboratory Standards Institute: Wayne, PA, USA, 2015.
61. Varela, A.R.; Ferro, G.; Vredenburg, J.; Yanik, M.; Vieira, L.; Rizzo, L.; Lameiras, C.; Manaia, C.M. Vancomycin resistant enterococci: From the hospital effluent to the urban wastewater treatment plant. *Sci. Total Environ.* **2013**, *450*, 155–161. [[CrossRef](#)] [[PubMed](#)]
62. Narciso-Da-Rocha, C.; Rocha, J.; Vaz-Moreira, I.; Lira, F.; Tamames, J.; Henriques, I.; Martinez, J.L.; Manaia, C.M. Bacterial lineages putatively associated with the dissemination of antibiotic resistance genes in a full-scale urban wastewater treatment plant. *Environ. Int.* **2018**, *118*, 179–188. [[CrossRef](#)] [[PubMed](#)]

